

Elastic Strain-Concentration Factor of Cylindrical Bars with Circumferential Flat-Bottom Groove under Static Tension

Hitham M. Tlilan

Abstract—Using finite element method (FEM), the elastic new strain-concentration factor (SNCF) of cylindrical bars with circumferential flat-bottom groove is studied. This new SNCF has been defined under triaxial stress state. The employed specimens have constant groove depth with net section and gross diameters of 10.0 and 16.7 mm, respectively. The length of flatness a_0 has been varied from 0.0 ~12.5 mm to study the elastic SNCF of this type of geometrical irregularities. The results that the elastic new SNCF rapidly drops from its elastic value of the groove with $a_0 = 0.0$, i.e. circumferential U-notch, and reaches minimum value at $a_0 = 2$ mm. After that the elastic new SNCF becomes nearly constant with increasing flatness length (a_0). The value of tensile load at yielding at the groove root increases with increasing a_0 . The current results show that severity of the notch decreases with increasing flatness length a_0 .

Keywords—Bar, groove, strain, tension

I. INTRODUCTION

THE structural and machine elements such as bars, axles, beam, etc. which are designed to avoid excessive elastic deflection, often fail suddenly by fracture. The presence of discontinuities or geometrical irregularities such as notches is a common reason for these failures. This is due to the amplification of the stress or strain amplitude at the boundaries of the geometrical irregularities. Moreover, the stress state is changed to be triaxial stress state at the immediate vicinity of the geometrical irregularities. Failure in machine elements takes place mainly at stress concentrations. Methods for predicting failure must take their effect into account. In design, it is common to use textbooks; [1], [2], to obtain the stress-concentration factor (SSCF). Also there have been many studies to tackle this problem, beginning with the work of Hardrath and Ohman, and Neuber [3],[4].

A considerable amount of work has been completed with regard to the determination of elastic stress concentration factor for common discontinuities or geometrical irregularities under static loading. Results of these studies have been presented in graphical representation of experimental results, empirical formulae, and in theoretical solutions [5] - [9]. Fewer studies have been done examining the SNCF of discontinuities under static loading. For static tension, it has been predicted by Neuber that the plastic SNCF increases and the plastic SSCF decreases from their elastic values as plastic

deformation develops from the notch root [2]. This prediction has been confirmed experimentally or analytically and given in literature [8]-[13]. These results indicate that for any type of loading, the SNCF is more important than the SSCF [14]-[19]. This is because the plastic SNCF maintains a high value much greater than unity, while the plastic SSCF decreases towards unity. The notches employed in the above studies are of intermediate depth, considered to give a strong notch effect.

A new SNCF has been defined under the triaxial stress state at the net section. This new SNCF provides reasonable values consistent with the concave distributions of the axial strain on the net section. Moreover, this new SNCF has removed the contradiction in the conventional SNCF having the values less than unity in spite of the concave distributions of the axial strain under elastic-plastic deformation. On the other hand, the conventional SNCF has been defined under the uniaxial stress state, which is completely different from the stress state at the net section, namely; the triaxial stress state [14]-[20]. This causes the above contradiction of the conventional SNCF. The SNCF for any type of loading must therefore be defined under the triaxial stress state at the net section. This is because the axial strain at the notch root occurs under the triaxial stress state SSCF [14]-[20]. The new SNCF has made it possible to clarify the strain concentration in notches under creep for the first time.

This paper attempts to improve the understanding of the effect flatness length (a_0) on the new SNCF for circumferential notches with flat bottom under static tension. The FEM is used to obtain the strain distributions. This study covers deformation level up to a deformation level close to where the notch tensile strength occurred.

II. NEW STRAIN-CONCENTRATION FACTOR

Recently, a new strain-concentration factor (SNCF) has been introduced by Majima for static tension [14]. This new SNCF is defined as the ratio of the maximum axial strain $(\varepsilon_z)_{\max}$ to new average axial or nominal strain at the net section $(\varepsilon_z)_{\text{av}}^{\text{new}}$;

$$K_{\varepsilon}^{\text{new}} = \frac{(\varepsilon_z)_{\max}}{(\varepsilon_z)_{\text{av}}^{\text{new}}} \quad (1)$$

The maximum axial strain at the notch root is independent of definition, and hence the new SNCF depends on the definition of the average axial strain. The axial strain is assumed to be uniformly distributed at the net section if the notch effect is negligible. This assumption gives the average axial or nominal strain. For circumferentially notched cylindrical bars $(\varepsilon_z)_{\text{av}}^{\text{new}}$ is defined as (14Majima 1999)

Hitham M. Tlilan is Assistant Professor in the Department of Mechanical Engineering, Faculty of Engineering in The Hashemite University Zarqa 13115, Jordan, (Tel. : +962-(0)5-3903333, Ext. (4463); Mobile: +962-(0)7-77368136 Fax: +962-(0)5-3826348; e-mail: hitham@hu.edu.jo).

$$\begin{aligned}
 (\varepsilon_z)_{av}^{new} &= \frac{1}{\pi r_n^2} \int_0^{r_n} \varepsilon_z(r) 2\pi r dr \\
 &= 2 \int_0^1 \varepsilon_z(s) s ds
 \end{aligned} \quad (2)$$

where $s = r/r_n$. In elastic deformation $(\varepsilon_z)_{av}^{new}$ can be transformed into

$$\begin{aligned}
 (\varepsilon_z)_{av}^{new} &= \frac{1}{\pi r_n^2} \int_0^{r_n} \left[\frac{\sigma_z}{E} - \frac{\nu}{E} (\sigma_\theta + \sigma_r) \right] 2\pi r dr \\
 &= \frac{1}{E \pi r_n^2} \int_0^{r_n} \sigma_z 2\pi r dr - \frac{\nu}{E \pi r_n^2} \int_0^{r_n} (\sigma_\theta + \sigma_r) 2\pi r dr \quad (3) \\
 &= \frac{P}{E \pi r_n^2} - \frac{\nu}{E \pi r_n^2} \int_0^{r_n} (\sigma_\theta + \sigma_r) 2\pi r dr \\
 &= \frac{(\sigma_z)_{av}}{E} - \frac{\nu}{E \pi r_n^2} \int_0^{r_n} (\sigma_\theta + \sigma_r) 2\pi r dr
 \end{aligned}$$

where E , ν and P are Young's modulus, Poisson's ratio and tensile load, respectively. Equation (3) can be rewritten as

$$(\varepsilon_z)_{av}^{new} = \frac{(\sigma_z)_{av}}{E} - \frac{2\nu}{E} \int_0^1 \{ \sigma_\theta(s) + \sigma_r(s) \} s ds \quad (4)$$

This equation indicates that $(\varepsilon_z)_{av}^{new}$ is defined under the triaxial stress state at the net section. It should be noted that $(\varepsilon_z)_{av}^{new}$, given by equation (2), is defined under the triaxial stress state also in plastically deformed area at the net section. This is because the plastic component of the axial strain is directly related to the triaxial stress state, as indicated by the theory of plasticity. The definition under the triaxial stress state gives the reasonable SNCF consistent with the concave distribution of the axial strain at any deformation level [14]-[20].

The conventional SNCF under static tension has been defined as the ratio of the maximum axial strain $(\varepsilon_z)_{max}$ at the notch root to the conventional average axial strain $(\varepsilon_z)_{av}^{con}$, i.e.

$$K_\varepsilon^{con} = \frac{(\varepsilon_z)_{max}}{(\varepsilon_z)_{av}^{con}} \quad (5)$$

The conventional average axial strain $(\varepsilon_z)_{av}^{con}$ has been given by the axial strain of an unnotched bar, which has the cross section identical with the net section and is subjected to the same load level as in the notched bar. This means that the conventional average axial strain $(\varepsilon_z)_{av}^{con}$ has been defined under the uniaxial stress state level [14]-[20]. In elastic deformation the conventional average axial strain $(\varepsilon_z)_{av}^{con}$ is given by the ratio of the average axial stress $(\sigma_z)_{av}$ ($= P /$ net section area) to Young's modulus E . Even in this stress range with plastic deformation at the notch root $(\varepsilon_z)_{av}^{con}$ has been given by

$$(\varepsilon_z)_{av}^{con} = \frac{(\sigma_z)_{av}}{E} \quad (6)$$

This equation indicates that the conventional definition has neglected the effect of the tangential stress σ_θ and the radial stresses σ_r . On further development of plastic deformation, i.e. in the range $(\sigma_z)_{av} > \sigma_Y$, $(\varepsilon_z)_{av}^{con}$ must be determined using

the uniaxial true stress-total strain curve $\sigma = f(\varepsilon)$. The conventional average axial strain is therefore given by

$$(\varepsilon_z)_{av}^{con} = f^{-1} \{ (\sigma_z)_{av} \} \quad (7)$$

III. MATERIALS AND GEOMETRIES

The material employed in this study is an Ni-Cr-Mo steel with tensile yield strength, Young's modulus, and Poisson's ratio of 525 (MPa), 206 (GPa), and 0.3, respectively. The true stress strain curves is obtained from conventional tension test.

Cylindrical bars with circumferential flat-bottom notches are employed in the current study, as shown in Fig. 1. Two different fillet radii 0.5 and 1.0 (mm) are employed. The gross and net-section diameters are 16.7 and 10.0 (mm),

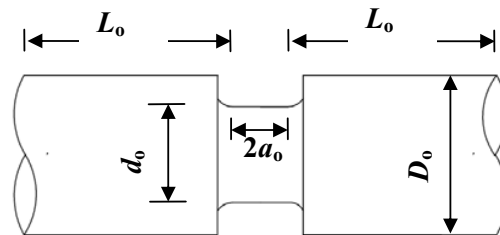


Fig. 1 Cylindrical bar with circumferential flat-bottom groove

respectively, to give net-to-gross diameter ratio of 0.6. In order to study the effect of flatness on the new SNCF, the gage length l_0 was kept constant of 50 mm and flatness length a_0 was varied from 0.0 to 12.5 (mm). It should be noted that $a_0 = 0.0$ (mm) expresses the circumferentially U-notched cylindrical bars.

IV. FINITE ELEMENT SIMULATIONS

Taking into account the symmetry of the specimens, only a quarter of the geometry was modeled. FE models of the employed specimen were constructed in the Marc code using 8-node axisymmetric isoperimetric quadrilateral ring element with biquadratic interpolation and full integration, type 28 in MARC classifications, is employed for tension in this study. A typical mesh of one-quarter for simulating the tensile loaded circumferentially notched bars is shown in Fig. 2. The meshes contain between 1717 and 15717 nodes, depending on the length of the specimen. A mesh-sensitivity analysis was conducted to investigate the influence of mesh discretization on the numerical observations. The mesh was varied by creating fine, moderate, and coarse models for all specimens employed. The FEM calculations were performed under the axisymmetric deformation, which is applied at the end of the unnotched part. The commercial finite element software, MSc Marc, was used for all calculations.

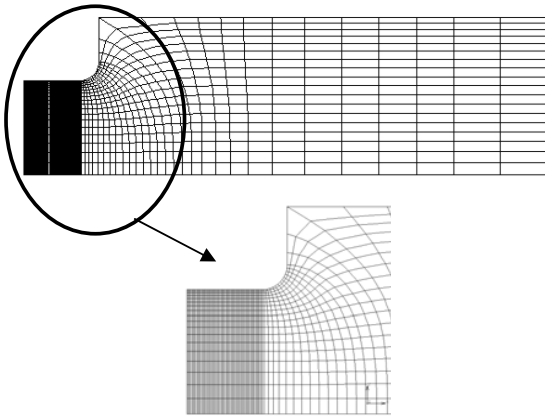


Fig. 2 FEM model of the circumferentially grooved Cylindrical bar.

V. RESULTS AND DISCUSSION

A. Variation in elastic new SNCF with tensile load

The variations of the elastic New SNCF with tensile load are plotted in Fig. 3 for all fillet radii and groove flattens lengths employed. It should be noted that the groove with zero flatness length is the circumferential U- notch (groove). As the tensile load increases the initial response is elastic and the SNCF is constant in elastic deformation. Figure 3 shows the effect of the flatness length on elastic new SNCF for all specimens employed. Elastic new SNCF in grooved specimens varies significantly with flatness length in the ranges where $a_o \leq 2$ mm, as clearly shown in Fig. 4. On the other hand, it becomes nearly independent of the flatness length in the range $a_o > 2$ mm. This is true for all groove and fillet radii employed. However, the maximum elastic SNCF of the circumferential U-groove, i.e. $a_o = 0.0$ mm, is greater than that of a groove with $a_o > 0.0$ mm. This indicates that the severity of the notch or groove vanishes with the presence of flatness length in the grooves. It vanishes also with increasing notch or fillet radius.

It is evident that there is notable influence of the flatness length as well as the fillet radius on elastic values and on the range of this constant value, i.e. elastic value of the new SNCF. Particularly, it increases with increasing flatness length in the range $a_o \leq 5$ mm, while it is independent of a_o in the range $a_o > 5$ mm. Also, this range increases with increasing notch or fillet radius. This can be clarified by plotting the relation between P_Y ; the tensile load value at yielding at the notch or fillet root, and flatness length a_o , as shown in Figures 5 and 6. It clearly shows that the value of P_Y rapidly increases with increasing a_o in the range $a_o \leq 2$ mm and slightly decreases with a_o up to $a_o = 5$ mm. After that P_Y becomes nearly independent of a_o .

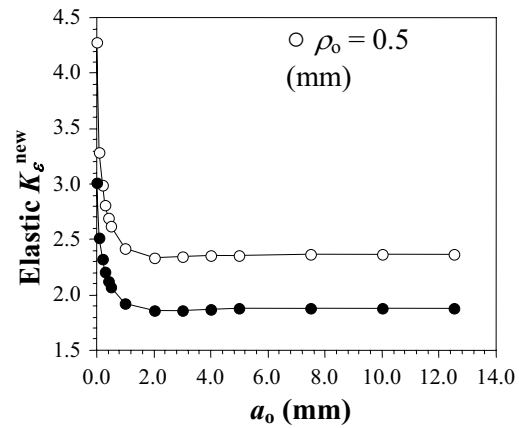


Fig. 3 Effect of flatness length on elastic new SNCF

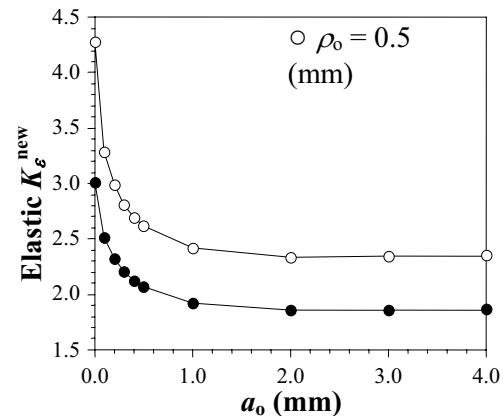


Fig. 4 Effect of flatness length on elastic new SNCF (enlarged)

Figure 7 shows the rapid decrease in the elastic new SNCF with increasing flatness length is essentially attributed to the decrease in the axial strain, i.e. maximum axial strain, at the notch or fillet root. This is prominent in the range where $0.0 < a_o \leq 2$ (mm), while it is nearly independent of a_o when $a_o > 2.0$ (mm). On the other hand, the average or nominal axial strain is nearly independent of a_o for all specimens employed. The current results showed that the strains were highest ahead of the notch root when the flatness is small, i.e. $0.0 < a_o \leq 2$.

VI. CONCLUSION

In the present work, FEM is used to study the elastic SNCF for circumferentially U- flat bottom notched bars in tension. The elastic SNCF rapidly decreases from its value at $a_o = 0.0$ (mm), i.e. circumferentially U-notch, to a minimum value at $a_o = 2.0$ (mm). For $a_o \geq 2.0$ the elastic SNCF is nearly independent of a_o . The range of elastic SNCF becomes larger with increasing a_o , i.e. the values of tensile load at yielding at the notch root P_Y , up to $a_o = 2.0$ (mm). For larger a_o , the values of P_Y are nearly independent of a_o .

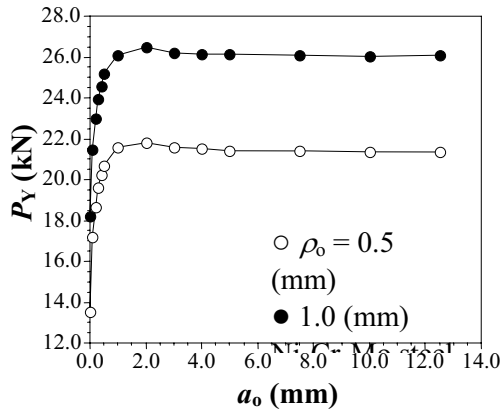


Fig. 5 Effect of flatness length on tensile load at yielding

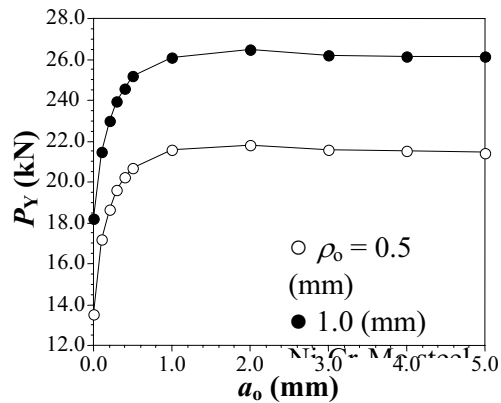
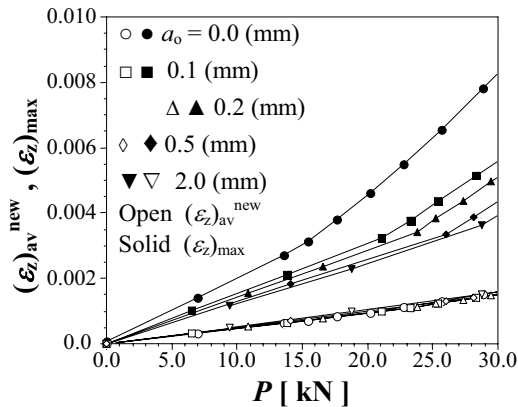


Fig. 6 Effect of flatness length on tensile load at yielding (enlarged)

Fig. 7 Variations in the $(\epsilon_z)_{av}^{new}$, $(\epsilon_z)_{max}$ with tensile load for Ni-Cr-Mo steel

REFERENCES

- [1] K. Nishida, Stress Concentration (in Japanese). Morikita Shuppan, Tokyo, 1974.
- [2] W.D. Pilkey, Peterson's Stress Concentration Factors. Wiley, New York, 1997.
- [3] H. F. Hardrath and L. Ohman, "A study of elastic and plastic stress concentration factors due to notches and fillets in flat plates," *NACA Report 1117*, National Advisory Committee Aeronautics, 1953.
- [4] H. Neuber, "Theory of stress concentration factor for shear-strained prismatical bodies with arbitrary nonlinear stress-strain law," *J. Appl. Mechanics*, vol. 28, pp. 544-550, 1961.

- [5] M. M. Leven and M. M. Frocht, "Stress-concentration factors for single notch in flat bar in pure and central bending," *J. Appl. Mechanics*, vol. 74, pp. 560-561, 1952.
- [6] A. Kato, "Design equation for stress concentration factors of notched strips and grooved shafts," *J. strain analysis*, vol. 26, pp. 21-28, 1991.
- [7] N. -A. Noda, M. Sera, and Y. Takase, "Stress concentration factors for round and flat test specimens with notches," *Int. J. Fatigue*, vol. 17 (3), pp. 163-178, 1995.
- [8] P.S. Theocaris, "Experimental solution of elastic-plastic plane stress problems," *J. Appl. Mechanics*, vol. 29, pp. 735-743, 1962.
- [9] P.S. Theocaris and E. Marketos, "Elastic-plastic strain and stress distribution in notched plates under plane stress," *J. Mech. Phys. Solids*, vol. 11, pp. 411-428, 1963.
- [10] A.J. Durelli and C.A. Sciammarella, "Elastoplastic stress and strain distribution in a finite plate with a circular hole subjected to unidimensional load," *J. Appl. Mechanics*, vol. 30, pp. 115-121, 1963.
- [11] P.S. Theocaris, "The effect of plasticity on the stress-distribution of thin notched plates in tension," *J. Franklin Inst.*, vol. 279, pp. 22-38, 1965.
- [12] K. Ogura, N. Miki, and K. Ohji, "Finite element analysis of elastic-plastic stress and strain concentration factors under plane strain and axisymmetric conditions (in Japanese)," *Trans. Japan Soc. Mech. Engrs.*, vol. 47, pp. 55-62, 1981.
- [13] S.J. Hardy and M.K. Pipelzadeh, "An assessment of the notch stress-strain conversion rules for short flat bars with projections subjected to axial and shear loading," *J. Strain Analysis*, vol. 31 (2), pp. 91-110, 1996.
- [14] T. Majima, "Strain-concentration factor of circumferentially notched cylindrical bars under static tension," *J. Strain Analysis*, vol. 34 (5), pp. 347-360, 1999.
- [15] H. M. Tlilan, N. Sakai, and T. Majima, "Strain-concentration factor of a single-edge notch under pure bending". (In Japanese) *Yamanashi District Conference*, No. 040-4, Japan, 2004
- [16] H. M. Tlilan, N. Sakai, and T. Majima, "Strain-concentration factor of rectangular bars with a single-edge notch under pure bending". (In Japanese), *Journal of the Society of Materials Science*, vol. 54 (7), 2005.
- [17] H. M. Tlilan, S. Yousuke, and T. Majima, "Effect of notch depth on strain-concentration factor of notched cylindrical bars under static tension", *European Journal of Mechanics A / Solids*, vol. 24 (3), 406-416, 2005.
- [18] H. M. Tlilan, N. Sakai, and T. Majima, "Effect of notch depth on strain-concentration factor of rectangular bars with a single-edge notch under pure bending", *International Journal of Solids and Structures*, vol. 43, 459-474, 2006.
- [19] H. M. Tlilan, A. S. Al-Shyyab, T. Darabseh, and T.Majima, "Strain-Concentration Factor of Notched Cylindrical Austenitic stainless Steel Bar with Double Slant Circumferential U- Notches Under Static Tension". *Jordan Journal of Mechanical and Industrial Engineering*, vol. 1(2), 105-111, 2007.
- [20] H. M. Tlilan, A. S. Al-Shyyab, A. M. Jawarneh, A. K. Ababneh, "Strain-concentration factor of circumferentially V-notched cylindrical bars under static tension". *Journal of Mechanics*, vol. 24 (4), 419-427, 2008.